

GT2011-453+\$

ULTRA HIGH BYPASS RATIO ENGINE SIZING AND CYCLE SELECTION STUDY FOR A SUBSONIC COMMERCIAL AIRCRAFT IN THE N+2 TIMEFRAME

**Brian K. Kestner
Jeff S. Schutte
Jonathan C. Gladin
Dimitri N. Mavris**

Aerospace System Design Lab
School of Aerospace Engineering
Georgia Institute of Technology
Atlanta, GA 30332

ABSTRACT

This paper presents an engine sizing and cycle selection study of ultra high bypass ratio engines applied to a subsonic commercial aircraft in the N+2 (2020) timeframe. NASA has created the Environmentally Responsible Aviation (ERA) project to serve as a technology transition bridge between fundamental research (TRL 1-4) and potential users (TRL 7). Specifically, ERA is focused on subsonic transport technologies that could reach TRL 6 by 2020 and are capable of integration into an advanced vehicle concept that simultaneously meets the ERA project metrics for noise, emissions, and fuel burn. An important variable in exploring the trade space is the selection of the optimal engine cycle for use on the advanced aircraft. In this paper, two specific ultra high bypass engine cycle options will be explored: advanced direct drive and geared turbofan. The advanced direct drive turbofan is an improved version of conventional turbofans. In terms of both bypass ratio and overall pressure ratio, the advanced direct turbofan benefits from improvements in aerodynamic design of its components, as well as material stress and temperature properties. By putting a gear between the fan and the low pressure turbine, a geared turbo fan allows both components to operate at optimal speeds, thus further improving overall cycle efficiency relative to a conventional turbofan. In this study, sensitivity of cycle design with level of technology will be explored, in terms of both cycle parameters (such as specific

thrust consumption (TSFC) and bypass ratio) and aircraft mission parameters (such as fuel burn and noise). To demonstrate this sensitivity, engines will be sized for optimal performance on a 300 passenger class aircraft for a 2010 level technology tube and wing airframe, a N+2 level technology tube and wing airframe, and finally on a N+2 level technology blended wing body airframe with and without boundary layer ingestion (BLI) engines.

INTRODUCTION

NASA's Environmentally Responsible Aviation (ERA) project funded under the Integrated Systems Research Program (ISRP) was created to conduct research at an integrated system level on promising concepts and technologies, as well as explore, assess, and demonstrate the benefits of chosen concepts and technologies in a relevant environment [1]. ERA's goal is to serve as a technology transition bridge between the lower TRL efforts on-going in the Fundamental Aeronautics program and potential users. Specifically, ERA is focused on subsonic transport technologies that could reach TRL 6 by 2020 and are capable of integration into an advanced vehicle concept that simultaneously meets the project metrics for noise, emissions, and fuel burn shown in Fig. 1. ERA has specified a 42 db reduction in cumulative noise compared to stage 4 noise stringency level [2].

CORNERS OF THE TRADE SPACE	N+1 = 2015*** Technology Benefits Relative To a Single Aisle Reference Configuration	N+2 = 2020*** Technology Benefits Relative To a Large Twin Aisle Reference Configuration	N+3 = 2025*** Technology Benefits
Noise (cum below Stage 4)	-32 dB	-42 dB	-71 dB
LTO NO _x Emissions (below CAEP 6)	-60%	-75%	better than -75%
Performance: Aircraft Fuel Burn	-33%**	-50%**	better than -70%
Performance: Field Length	-33%	-50%	exploit metro-plex* concepts

***Technology Readiness Level for key technologies = 4-6
 ** RECENTLY UPDATED. Additional gains may be possible through operational improvements
 * Concepts that enable optimal use of runways at multiple airports within the metropolitan area

FIGURE 1. ERA METRIC GOALS [1]

The project has established a set of technologies and concepts for which system level analysis is needed to quantify the feasibility, benefits, and risks associated with simultaneously achieving the ERA metrics for commercial aviation.

Previous System Studies

Over the past 10-20 years, there have been numerous ultra high bypass engine studies. In the early 1990s, GE conducted a study estimating 2005 technology level performance of a geared turbofan and advanced direct drive engine applied to a 250-300 pax airframe [3]. In 2003, Boeing conducted a similar study which estimates 2015 technology level performance of an advanced direct drive and geared turbofan engines applied to 300 pax aircraft [4]. In this study it was concluded that a geared turbofan can provide a 2% better fuel reduction relative to an advanced direct drive. Boeing also conducted an advanced engine performance study for advanced tube and wing as well as blended wing body aircraft [5]. In this study, a fixed advanced engine was applied to advanced aircraft of different passenger classes. It was stated in this study that it was unknown whether the engine used for the blended wing body aircraft was optimal in terms of fuel burn. More recent studies by Cambridge University and MIT under the Silent Aircraft Initiative evaluated different engine configurations as well as engine cycles [6] [7] [8] [9]. In these studies, different considerations regarding fan pressure ratio selection, variable nozzle scheduling, LPT design, and transmission design were discussed. In 2009, NASA performed engine concept studies estimating of 2015 level technology level performance of an advanced direct drive and geared turbofan engines for both a hybrid wing body and a tube and wing body [10] [11]. The purpose of this current study is to bring together the information from these previous studies as well as understand how the engine design will change with the inclusion of different airframe and engine technologies expected to mature in the N+2 timeframe.

Technologies to be Assessed

In its ERA workplan, NASA has identified numerous technologies that have the potential to mature in the N+2 time frame [12]. These technologies have been grouped into different categories for airframes, engines and vehicle integration. The airframe technology focus is on lightweight structures, drag reduction and noise reducing technologies. Technologies in this category include the Pultruded Rod Stitched Efficient Unitized Structure (PRSEUS), hybrid and laminar flow control technologies and landing gear fairings. The engine technologies are focused on higher OPR and T4 core technologies, higher propulsor efficiency and low NO_x combustors technology. Engine technologies developed within ERA include active flow control, active film cooling, and highly loaded components [13] as well as ceramic matrix composite material technologies [14]. In addition to specific technologies, certain advanced airframe and engine configurations are being explored. On the airframe side advanced tube and wing as well as hybrid wing body are being considered. The hybrid wing body concept offers potential fuel burn reduction of 15% relative to a comparable tube and wing concept. The advanced direct drive and geared turbofan were applied to both airframes. The advanced direct drive is an improved version of today's conventional turbofans in terms of overall pressure ratio, turbine inlet temperature, and component efficiency [15]. A geared turbo fan is meant to further improve upon the concept of a turbofan by allowing the fan and low pressure systems to operate at different speed, thus improving the efficiencies of the LPT [16] [17] and allowing for higher BPR improving engine propulsive efficiency.

METHODOLOGY

The Environmental Design Space (EDS) is a tool developed for the U.S. Federal Aviation Administration's Office of Environment and Energy (FAA/AEE) as part of a comprehensive suite of software tools that allows for a thorough assessment of the environmental effects of aviation [18]. EDS provides the capability to generate an integrated analysis of aircraft performance, source noise, and exhaust emissions at the aircraft level for potential future aircraft designs under different policy and technological scenarios. The integrated analysis enables the assessment of the interdependencies and associated trade-offs between aircraft performance, noise and emissions in a transparent and traceable manner.

EDS is a physics-based, integrated, multidisciplinary modeling and simulation environment that seamlessly combines core EDS modules originally developed by NASA coupled with design rules and logic along with user defined engine and airframe design parameters to create aircraft designs. The basic flow of information during the execution of EDS for a single aircraft is shown in Figure 2. The primary modules cover engine design using CMPGEN [19] [20] for compressor map generation, NPSS

[21] [22] for thermodynamic cycle analysis and WATE [23] [24] for engine flow path analysis and weight estimation, vehicle sizing and synthesis with FLOPS [25], emissions based on correlations derived from the P3-T3 method [26], and aircraft noise using ANOPP [27] [28]. The EDS environment is structured using the object-oriented code used to power NPSS, allowing information to be passed between the EDS modules and then executed in an automated fashion to ensure that analysis results are consistent with the produced vehicles.

The EDS environment can be thought of as executed in four phases for a single vehicle. Phase 1 is the EDS initialization phase which establishes the different options for running EDS and determines the settings of all of the design variables. Phase 2 is the vehicle design phase which sizes both the engine and airframe. In this phase, there is first a design loop for the engine and then a design loop between the engine and airframe. The engine design loop first performs the thermodynamic cycle design at the aerodynamic design point; integrating a multi-point design methodology to ensure the engine meets thrust requirements at both top of climb (TOC) and take-off [29]. There are then iterations between the thermodynamic cycle design and the flow path analysis until the two analyses converge. After completion of the engine design loop, the vehicle design loop starts by running the thermodynamic cycle model in off-design mode throughout the flight envelope to generate an engine deck for the aircraft mission analysis. The aircraft mission analysis is run for a given mission, payload, thrust to weight ratio, and wing loading, scaling the engine deck thrust and the vehicle size to meet the targets. If the engine deck thrust is scaled, the engine design loop is executed again with the new thrust targets. This loop is repeated until the engine does not scale in the aircraft mission analysis. The vehicle is fixed at the end of this phase. The third phase is the vehicle performance evaluation phase. In this phase all desired performance evaluation is conducted including gaseous emissions, noise certification, takeoff and landing performance, and fuel burn for off design points on a payload-range chart. Phase 4 is the output data phase. Here all desired data is compiled into user specified summary files.

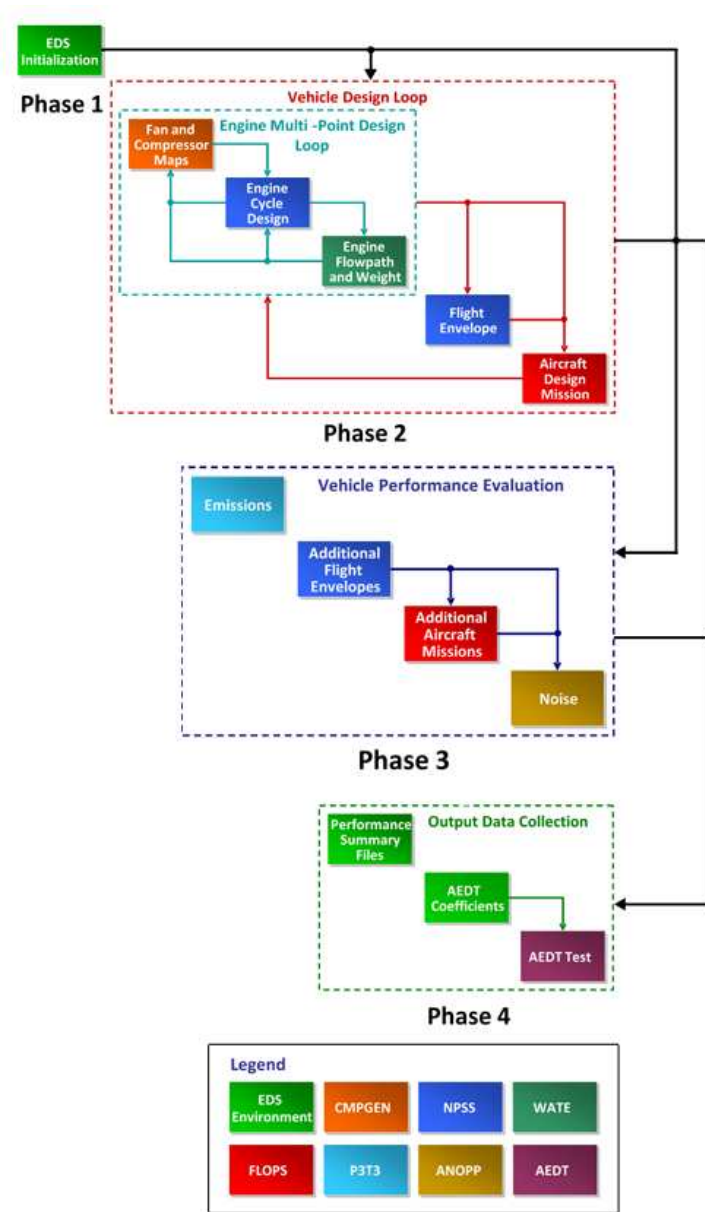


FIGURE 2. EDS FLOW CHART

ADVANCED ENGINE CYCLE DESIGN

The baseline engine model for the 300 passenger aircraft is the General Electric GE90-94B. The goal of the advanced cycle development is to upgrade this existing engine model to an advanced cycle representative of newer engine technology and more advanced architectures such as the geared turbofan, both of which represent potential improvements in TSFC as well as fuel burn and noise with respect to conventional designs. The essential difference between the advanced direct drive turbofan and conventional models is the improvement of overall pressure ratio, and the lowering of fan pressure ratio in order to increase propulsive efficiency relative to conventional designs. An exam-

ple of such a technology includes the GENx engine being developed by GE-Aviation, which will be used as a calibration point in this development.

The development of OPR over the last few decades for multiple jet engine manufacturers is shown in Fig. 3. This upward trend has been driven primarily by improvements in material temperature limits at the compressor exits which allow for much higher burner entrance temperatures as well as improvements in compressor performance. With increased OPR, there is

also an increase in thermal efficiency and corresponding reduction in TSFC and fuel burn [30], which is a driving motivation for this study. The current 2010 maximum OPR is 43; this is the value to be used for the 2010 level advanced and geared turbofan cycles. Using Fig. 3 as a guideline, the anticipated OPR for the 2020 N+2 simulations is conservatively estimated at approximately 46 which is lower than other N+2 studies [7].

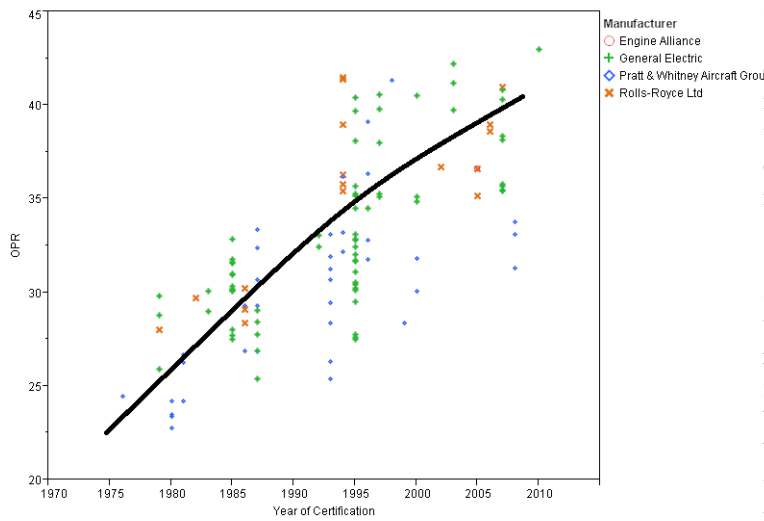


FIGURE 3. COMMERCIAL ENGINE OPR HISTORY

The next step is to determine an appropriate value for the HPC pressure ratio. The GENx engine will have a similar compressor to the GE90, with an HPC pressure ratio of 23 [31]. Once overall and compressor pressure ratio are determined for the advanced cycle, then the low pressure compressor and fan pressure ratios are bound by a fixed ratio with respect to each other. Therefore choosing a FPR in effect chooses LPCPR, in order to maintain the chosen values of OPR and HPCPR. Although FPR will be used as an independent variable in the cycle selection trade study, a somewhat arbitrary value of 1.5 will be chosen to create the baseline advanced cycle. Accordingly, the LPCPR falls out when taking account of pressure losses in the ducts between the compressor elements. Given the HPC pressure ratio, the HPC loading is increased to match the GENx HPC stage count of 10 [31]. Such a low stage count is possible due to a steady increase in maximum per stage loading, facilitated by innovations in aerodynamic analysis and design as well as the use of advanced materials [30], which thereby eliminates the weight penalty conventionally incurred by increased HPCPR.

For all the test cases, the turbine inlet temperature was held constant. Thus when technologies such as CMC blades and vanes or improved film cooling are applied, the resultant en-

gine cycle will have a reduction in the amount of turbine cooling flows. Values for the LPC, Fan, and HPC polytropic efficiencies and HPT adiabatic efficiency are quoted in [10] and are estimates of 2015 component performance. The LPT adiabatic stage efficiency is a function of the LPT loading and flow coefficient using curves defined by Aungier [32]. The LPT stage count is calculated within the EDS environment and is a function of LPT loading. The GENx LPT stage count is 6 stages and is therefore a general target for the LPT [31]. The HPT stage count is an input, and is held at 2 stages, consistent with the GENx HPT.

As fan aerodynamic and material designs improve, the necessary blade count to achieve a specific pressure ratio while maintaining efficiency is reduced. This leads to significant weight savings and must therefore be captured by the advanced cycle development process. The blade count of the baseline model was therefore reduced from 22 to 18 and the associated solidity factors were reduced accordingly.

Finally, the cycle design must be completed by determining appropriate values for FPR, extraction ratio, and LPT loading for the direct drive engine. For the geared turbofan model, the gear ratio is added as an additional independent variable. A space filling latin hypercube design of experiments was constructed for both the GTF and direct drive advanced cycles to determine the best fuel burn settings. For each test case 567 design settings were analyzed with 359 settings for the GTF and 208 settings for the direct drive. Table 1 shows the ranges for each design variable. Because of the higher rotational speed of the LPT on the GTF, the range of LPT loading for the GTF was at lower values than for the DDTF. The results of these experiments will be covered in the next section.

TABLE 1. RANGES OF DESIGN VARIABLES IN LATIN HYPER-CUBE DOE

	DDTF		GTF	
	min	max	min	max
FPR	1.4	1.6	1.35	1.6
LPT Loading	1.5	2.1	1	1.5
Extraction Ratio	1	1.3	1	1.3
Gear Ratio	NA	NA	2	3

TEST CASES

There are five test cases that are used to demonstrate the change in engine performance with respect to different technologies, engine architecture, and airframe architecture. The first case that will be examined is a 2010 engine and airframe technology on a tube and wing aircraft. The second test case is N+2 level engine and airframe technologies, applied to a tube and wing aircraft. The third test case examined is N+2 engine

TABLE 2. BASELINE 300 PAX PERFORMANCE

FPR	1.58
BPR	8.80
TSFC	0.5363
Engine Diameter	123
SLS Thrust	97300
Engine Weight	16658
LPC stages	3
LPT stages	6
Fuel Burn	246329
Stage IV Noise Margin	11.2
TOGW	656000
OEW	320800

and airframe technologies applied to a HWB aircraft with podded engines. The fourth and fifth test cases are N+2 engine and airframe technologies applied to a HWB aircraft with boundary layer ingestion (BLI) engines. The difference between these two BLI cases is in the first case the engine is flush mounted on the airframe while in the second case the engine is embedded in the airframe. In addition to demonstrating the effects of boundary layer ingestion, these cases can be used to highlight the sensitivity of vehicle performance with respect to assumptions made on cycle performance. All the N+2 test cases analyzed below contain only one of the 1800 technology combinations used in ERA vehicle assessment [33]. For all the subsequent figures below, the test points with diamonds represent a direct drive turbofan (ddtf) engine while the circles represent a geared turbofan (gtf) engine.

Before the results of the test cases are analyzed, an appropriate baseline has to be defined. As mentioned previously, the GE90-94B represents the baseline engine configuration while the representative airframe is the Boeing 777-200ER with a payload of 301 seats. The design mission for the vehicle from the fuel burn is calculated is 7440 nautical miles. Below in Tab. 1 are some baseline performance figures for the 300 pax aircraft. These values can be used as a reference throughout the rest of the paper.

2010 Tube and wing

The 2010 tube and wing aircraft configuration has improvements to both the engine and aircraft relative to the baseline engine. Technologies such as composites were applied to the airframe wings while improved component aerodynamics and fan design were applied to the engines.

The raw data scatter plot from the Latin hypercube design of experiments for the 2010 technology level is shown in Fig. 4 with noise margin on the horizontal axis and overall fuel burn on the vertical axis. The solid curve shown is the outline of the Pareto curve for this set of data, which is the curve that defines all of the potential "best" solutions from the data set. All points above this curve are dominated by some solution on the curve. Figure 4 shows that the minimum fuel burn for the geared turbo

fan has approximately a 3% lower fuel burn than the DDTF while the maximum noise margin is about 2 dB higher. Note that this is not true for every design, since some GTF cases are actually above the DDTF Pareto curve, but in general these trends reflect the paradigm shift that the GTF technology represents for high by-pass ratio turbofans.

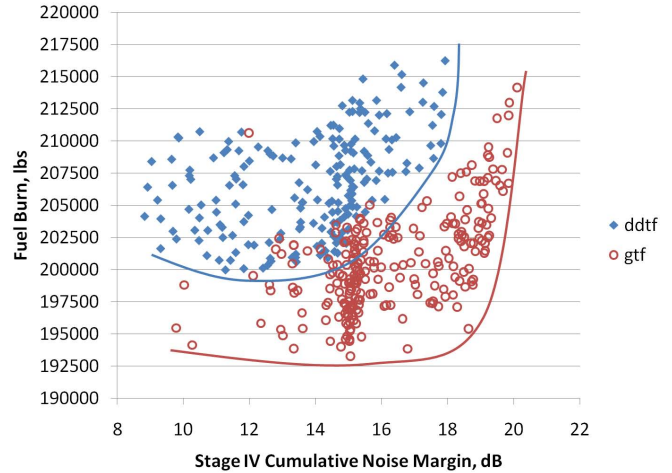


FIGURE 4. 2010 TUBE AND WING PERFORMANCE VERSUS ERA METRICS

TABLE 3. 2010 TUBE AND WING PERFORMANCE

	Direct Drive			Geared Turbofan		
	FPR	1.402	1.496	1.559	1.353	1.415
BPR	14.05	11.45	9.96	17.37	14.72	12.60
TSFC	0.5023	0.5082	0.5164	0.4977	0.492	0.5008
Engine Diameter	137.3	123.5	116.5	146.4	132.3	124.2
SLS Thrust	84960	81385	80322	83142	79307	78517
Engine Weight	19253	15225	13467	17182	14223	12662
LPC stages	3	3	2	2	2	2
LPT stages	10	8	7	3	4	3
Gear Ratio	1	1	1	2.88	2.19	2.09
Fuel Burn	209812	201287	200072	206721	193853	193270
Stage IV Noise Margin	17.8	14.7	11.8	19.8	16.8	15.1
TOGW	573354	547286	539237	563363	534809	528085
OEW	278534	261889	255182	272074	257780	251712

Since the goal of the ERA project is to simultaneously meet noise and fuel burn metrics, the engine cycle can be used as an additional technology knob. If a certain metric cannot be met, the design engine cycle may be changed to help improve it. However, as seen from the shape of the Pareto curve, there is a tradeoff between noise and fuel burn, where an increase in one will gen-

erally result in a decrease in the other. From each Pareto curve, there has been selected 3 points of interest which will be defined as follows for both the DDTF and GTF: the far left column is the "Best Noise"; the middle column is the "Compromise"; and the far right column is the "Best Fuel". The "Compromise" case was chosen to have the maximum noise margin that is within 1% fuel burn of the minimum fuel burn. These cases are shown in Table 3 with the various cycle and vehicle performance parameters associated with each case. Using these points, relative to the baseline, the GTF can obtain up to 20% reduction in fuel burn or approximately 12 dB reduction in cumulative noise, while the direct drive offers up to 15% reduction in fuel burn or approximately 12 dB in cumulative noise.

The first trend of importance to note is the variation of fuel burn and BPR with FPR. As FPR falls, there is a general increase in BPR and a decrease in TSFC associated with the increased propulsive efficiency of the cycle. This generally leads to a decline in total fuel burn with a decrease in FPR. However, the smaller FPR has two counteracting factors to overall fuel burn. The first is that the specific thrust tends to decrease with a decreasing FPR, requiring the engine to have larger diameters to meet thrust and therefore produce more nacelle drag; the second is that the increased fan and engine size generally lead to heavier total engine weight. This leads to a larger thrust requirement in the mission analysis and necessitates the scaling of the engine thrust in the engine design loop, which in turn requires the scaling of the entire vehicle to maintain the thrust to weight design point. The net result produces a somewhat second order trend which places the minimum fuel burn at FPR = 1.559 for DDTF, and FPR = 1.462 for the GTF. Note that, in general, decreasing FPR tends to decrease TSFC for high by-pass ratio turbofans; however the "Best Noise" case for the GTF was near the boundary of the design space explored and the Latin hypercube DOE did not sample a test point that resulted in lower TSFC than the "Compromise" case.

Additionally, the OEW and TOGW tend to trend similarly with fuel burn, since the vehicle is being scaled at higher diameter configurations. Table 3 shows that lowering FPR is shown to have a direct effect on reducing the cumulative noise margin. Also, the GTF configuration has a LPT stage count which is independent of FPR, since the gear ratio can be used to allow for higher speed LPT's which operate at higher efficiencies and weigh less due to a decrease in stage length and blade count.

N+2 Tube and Wing

The N+2 tube and wing aircraft configuration represents the further inclusion of other airframe and engine technologies relative to the 2010 aircraft. Some of these technologies were mentioned earlier in the paper. For this and all other cases using N+2 level technologies, a single representative subset of the technologies are applied. The final selection of which technologies should

be applied to a N+2 aircraft to best meet all the performance goals is beyond the scope of this paper.

Figure 5 shows the scatter plot and Pareto curves for the N+2 level technology aircraft. The trends noted in the 2010 level technology aircraft are similar where fuel burn increases and cumulative noise decreases as FPR decreases. Similar to the 2010 level trends, the GTF offers approximately 3% lower fuel burn relative to a direct drive engine for the best fuel burn case.

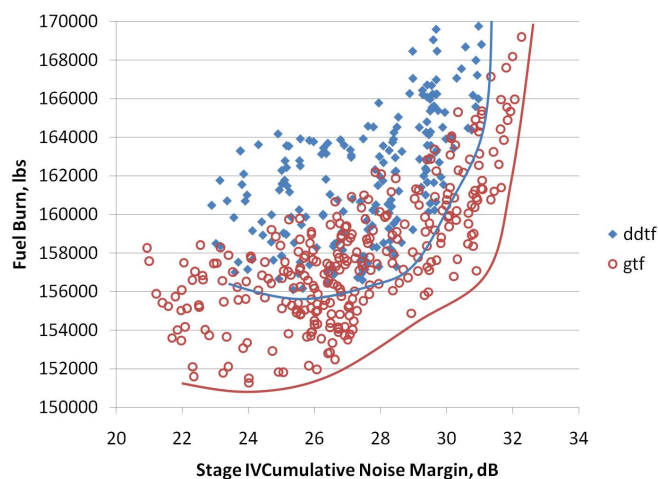


FIGURE 5. N+2 TUBE AND WING PERFORMANCE VERSUS ERA METRICS

TABLE 4. N+2 TUBE AND WING PERFORMANCE

	Direct Drive			Geared Turbofan		
	1.403	1.492	1.587	1.36	1.462	1.565
FPR	16.85	14.07	11.91	20.00	15.10	12.69
BPR	0.50	0.5034	0.511	0.4965	0.499	0.5047
TSFC	127.9	115.9	108.2	134.6	116.3	108.4
Engine Diameter	71992	68968	68110	70800	67109	66278
SLS Thrust	14369	11304	9732	12925	9463	8456
Engine Weight	4	3	3	3	2	2
LPC stages	12	10	8	4	4	3
LPT stages	1	1	1	2.92	2.09	2.06
Gear Ratio	164361	157281	156083	161390	152479	151268
Fuel Burn	30.8	28.5	25.3	31.7	26.6	24.0
Stage IV Noise Margin	484803	464768	457410	476922	452664	447214
TOGW	239586	227465	221482	235007	220754	216677
OEW						

Table 4 summarizes the results for the "Best Fuel", "Compromise", and "Best Noise" cases as done for the 2010 study. The inclusion of the N+2 technologies results in further increases in the BPR for both the direct drive and GTF engines, as well as associated decreases in fuel burn, OEW, and TOGW. Even though

the BPRs have increased across the board, the engine diameters have actually decreased because of the inclusion of drag reduction technologies. The noise margins have increased due to the addition of N+2 level noise technologies, but in this case, the "Best Noise" GTF provides a 50% smaller increase in noise margin (1dB). For both the "Compromise" and "Best Fuel" cases, the noise margin on the GTF is lower by about 1-2 dB than the corresponding DDTF. Even though the DDTF "Compromise" and "Best Fuel" cases have better noise margins than the corresponding cases for the GTF, a design compromise could be made such that the GTF could meet any target for noise margin that the DDTF could offer while still providing a significant fuel burn reduction. This is more clearly reflected by comparing the Pareto Curves in Fig. 5. Picking a point on the GTF Pareto curve that matches the DDTF best compromise noise margin still results in a 1.5% reduction in fuel burn relative to the DDTF. For this GTF cycle, the FPR is 1.415, BPR is 17.39, and the TSFC is 0.4933.

N+2 Hybrid Wing Body With Podded Engines

The hybrid wing body aircraft has the potential to offer further fuel burn and noise reductions relative to the more traditional tube and wing aircraft due to improved aerodynamic performance and noise shielding [34]. This test case explored the engine performance on a HWB aircraft with an identical set of technologies as used on the previous case. Fig. 6 shows the scatter plot matrix and Pareto curves associated with the podded engine configuration for the DDTF and GTF. The trends of fuel burn and noise with respect to FPR are the same as observed for the tube and wing case, as are the typical improvements of the GTF engine over the DDTF. The engine configurations for the podded HWB and tube and wing produce similar trends for the cases close to the Pareto frontier as seen in comparing figures 5 and 6. In this case, the GTF provides a 3.5% potential fuel reduction and 0.5 dB noise margin increase relative to the best cases for the DDTF.

Moreover, many of the cycle values shown in table 5 for the three cases of interest are remarkably close given the vast differences in the aircraft. Similar to the N+2 tube and wing analysis, taking the "Compromise" solution from the DDTF data, and finding the GTF point which matches that noise margin, the GTF can provide an additional 1.87% fuel reduction while matching the DDTF noise margin. The cycle values for this compromise case are FPR of 1.424, BPR of 16.68, and TSFC of 0.5012.

N+2 Hybrid Wing Body With Boundary Layer Ingestion Engines

For the HWB aircraft there is further opportunity for fuel burn reductions by placing the engines in the boundary layer of the aircraft. This allows for ram drag reduction by the engines ingesting the lower momentum boundary layer as well reduction of the viscous drag of the airframe because of reduced wet-

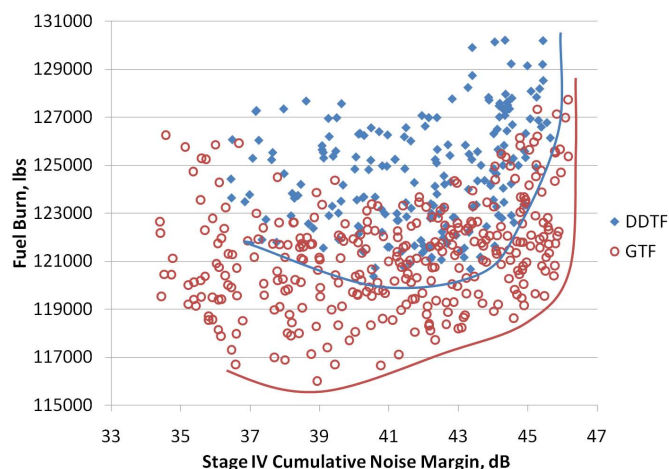


FIGURE 6. N+2 HWB WITH PODDED ENGINES PERFORMANCE VERSUS ERA METRICS

TABLE 5. N+2 HWB WITH PODDED ENGINES PERFORMANCE

	Direct Drive			Geared Turbofan		
FPR	1.403	1.482	1.587	1.353	1.462	1.565
BPR	16.88	14.22	11.80	20.29	14.95	12.48
TSFC	0.5033	0.5056	0.5134	0.506	0.5021	0.5074
Engine Diameter	112.9	103.5	95.5	121.2	103	95.8
SLS Thrust	55980	54488	53611	55818	53088	52586
Engine Weight	10588	8560	7261	9955	7196	6451
LPC stages	4	3	3	3	2	2
LPT stages	12	10	8	3	4	3
Gear Ratio	1	1	1	2.88	2.09	2.06
Fuel Burn	126139	121178	120371	125370	117723	116011
Stage IV Noise Margin	45.6	43.6	40.6	46.2	42.3	38.9
TOGW	416236	402859	398317	412732	394574	389661
OEW	213536	205666	202047	210814	201289	198245

ted area [5]. However, there are potential adverse effects from boundary layer ingestion. The ingesting of the boundary layer results in a lower engine inlet pressure which reduces the engine thermal efficiency. There may also be additional losses because of mixing or, for embedded engine in particular, the use of a large S-duct inlet. These additional pressure losses in the duct may be on the order of 1-2% [5] [6]. Additionally, the non-uniform flow in the inlets may result in reductions in fan efficiency and stall margin. Technologies such as inlet flow control and 3-D aerodynamics can aid in reducing and even potentially eliminating some of adverse effects on the fan [35]. Two boundary layer ingestion cases are explored in this paper: flush mounted engines and embedded engines. The lower momentum inlets for the engine resulting from boundary layer ingestion were modeled in

a similar fashion as that of NASA N+3 BLI studies [36]. BLI engines may have additional noise benefits due to the increased effectiveness of shielding. However, this effect was not accounted for in these simulations.

Figure 7 shows the Pareto curves of the DOE for the flush mounted engine with a BLI engine. To estimate the effects of mixing of the boundary layer and freestream flows, the BLI inlet was assumed to have a 1% higher total pressure drop relative to the podded engine case. In this case, the GTF provides a 3.1% fuel burn reduction and 0.5 dB noise margin increase relative to the respective best cases for the DDTF. Taking the "Compromise" solution from the DDTF data, and finding the GTF point which matches that noise margin, the GTF can provide an additional 2.4% fuel reduction while matching the DDTF noise margin. This means that the GTF improvement over the DDTF for the same noise margin actually increases by mounting the engine flush with the fuselage. The cycle for this compromised case is a FPR of 1.453, BPR of 14.97, and a TSFC of 0.5029.

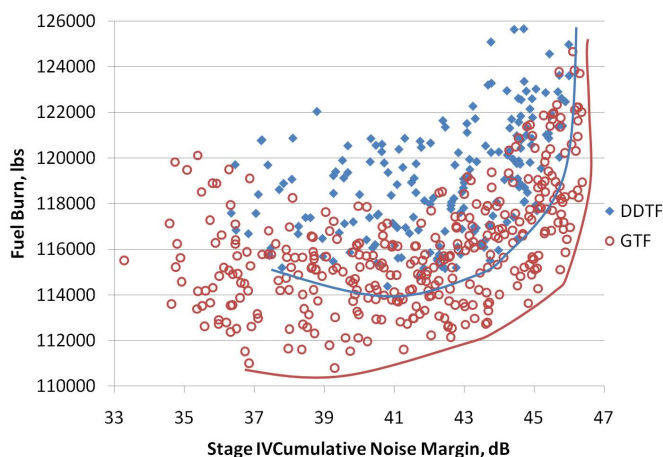


FIGURE 7. HWB WITH FLUSH MOUNTED ENGINES PERFORMANCE VERSUS ERA METRICS

Embedding the engine in the airframe reduces the overall drag because of a decrease in the wetted area of the nacelle. However, embedding the engine may require the use of a large S-duct inlet which may increase the pressure drop across the inlet. To estimate this effect, all the embedded engine test points were simulated with an additional 1% total pressure drop across the inlet relative to the flush mounted engines. Figure 8 shows Pareto curves of the DOE for the embedded engine with BLI. In this case, the GTF provides a 3.6% fuel burn reduction and 0.5dB noise margin increase relative to the respective best cases for the DDTF. Taking the "Compromise" solution from the DDTF data,

TABLE 6. HWB WITH FLUSH MOUNTED ENGINES PERFORMANCE

	Direct Drive			Geared Turbofan		
FPR	1.407	1.492	1.587	1.36	1.462	1.565
BPR	16.09	13.44	11.25	19.24	14.37	11.90
TSFC	0.5139	0.5049	0.5127	0.503	0.5026	0.5067
Engine Diameter	113.7	102.2	94.8	119.1	102.7	95.3
SLS Thrust	55626	53573	52750	54475	52363	51742
Engine Weight	10529	8477	7268	9697	7190	6399
LPC stages	4	3	3	3	2	2
LPT stages	10	10	8	4	4	3
Gear Ratio	1	1	1	2.92	2.09	2.06
Fuel Burn	123608	115507	114378	118938	112150	110802
Stage IV Noise Margin	46.0	43.7	40.8	46.4	42.6	39.3
TOGW	413531	396204	391020	404736	387814	383603
OEW	212947	204749	200871	209367	200155	197476

and finding the GTF point which matches that noise margin, the GTF can provide an additional 1.4% fuel reduction while matching the DDTF noise margin. This means that the GTF improvement over the DDTF increases for the best case, but actually decreases in the case where a noise compromise is reached between the DDTF and GTF. The cycle for this compromised case is a FPR of 1.464, BPR of 14.7, and a TSFC of 0.5171.

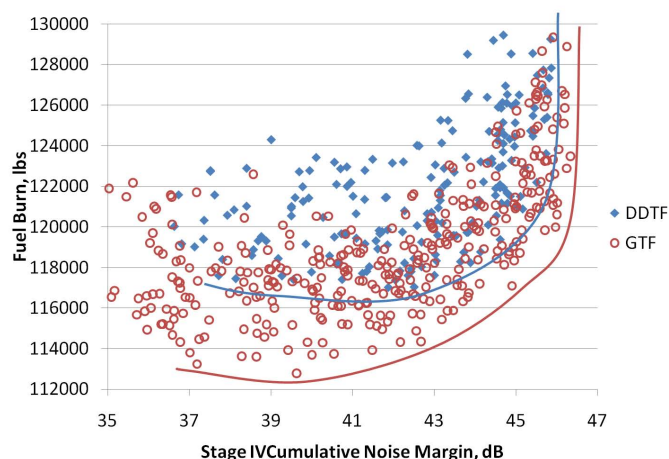


FIGURE 8. HWB WITH EMBEDDED ENGINES PERFORMANCE VERSUS ERA METRICS

Summary of Test Cases

Tables 8 and 9 summarize the differences between each case for the direct drive and GTF engine, respectively. From the base-

TABLE 7. HWB WITH EMBEDDED ENGINES PERFORMANCE

	Direct Drive			Geared Turbofan		
FPR	1.407	1.492	1.523	1.36	1.462	1.565
BPR	16.00	13.34	12.33	19.09	14.28	11.84
TSFC	0.5267	0.515	0.5186	0.5176	0.513	0.5152
Engine Diameter	116.1	103.7	100.2	121.8	104.2	96.7
SLS Thrust	56667	53998	53576	55515	52828	52303
Engine Weight	11110	8794	8073	10143	7422	6605
LPC stages	4	3	3	3	2	2
LPT stages	10	10	9	3	4	3
Gear Ratio	1	1	1	2.92	2.09	2.06
Fuel Burn	127838	118232	117035	123491	114353	112786
Stage IV Noise Margin	45.9	43.9	42.5	46.3	42.7	39.6
TOGW	421393	401240	396931	412628	391406	387076
OEW	215733	206470	203530	211799	201007	198515

line to the 2010 level technology, there is an increase in OPR which leads to a higher BPR, lower TSFC, fuel burn, and empty weight. Additionally, adding the N+2 technologies to the tube and wing configuration allows for higher OPR due to the increase in the allowable temperature of the high pressure compressor. However, many of the noise technologies used in this study require cycle bleed penalties which degrade the overall TSFC, which is why TSFC actually increased going from 2010 to the N+2.

Going from the tube and wing configuration to the HWB podded configuration does not have much effect on the engine cycle performance, as most of the cycle metrics did not significantly change. However, the important effects captured here are the gains made in the metrics by the change to the revolutionary HWB concept. The first point to note is the somewhat expected increase in noise margin: for the best noise N+2 cases, the increase in cumulative noise margin is a significant 15 dB. Furthermore, similar improvements are seen with respect to mission fuel burn and OEW with 23% less fuel burn and 8.3% less empty weight. Relative to the baseline, the HWB offers close to a 50% reduction in fuel burn or up to 40 dB reduction in engine noise.

The addition of boundary layer ingestion with flush mounted engines does not degrade TSFC much, since the loss in inlet pressure recovery is countered by the decrease in ram drag associated with ingesting the boundary layer. Additionally, flush mounting the engine allows for lower nacelle drag since the total wetted area of the airframe is reduced. The net effect of these three phenomena is to improve fuel burn relative to the podded case by 4.7%. For the case of the embedded BLI engine, the pressure drop was increased by 1% across the inlet. This results in a slightly higher TSFC relative to the flush mounted case because of the degraded thermal efficiency and the fact that there are no further reductions in ram drag by embedding the engine. The nacelle drag is diminished since the total wetted area of the nacelle is further reduced by embedding the engine. The net effect is that the fuel burn for the embedded case is approximately 2.5% better

than the podded case, but is still worse than the flush case. These results stress the critical importance of designing low pressure loss inlets for the BLI configuration.

TABLE 8. ADVANCED DIRECT DRIVE ENGINE PERFORMANCE

	Baseline	2010	N+2 Tube and Wing	N+2 HWB with Podded Engines	N+2 HWB with Flush Mounted BLI Engines	N+2 HWB with Embedded BLI Engines
FPR	1.58	1.496	1.492	1.482	1.492	1.492
BPR	8.80	11.45	14.07	14.22	13.44	13.34
TSFC	0.5363	0.5082	0.5034	0.5056	0.5049	0.515
Engine Diameter	123	123.5	115.9	103.5	102.2	103.7
SLS Thrust	97300	81385	68968	54488	53573	53998
Engine Weight	16658	15225	11304	8560	8477	8794
LPC stages	3	3	3	3	3	3
LPT stages	6	8	10	10	10	10
Gear Ratio	1	1	1	1	1	1
Fuel Burn	246329	201287	157281	121178	115507	118232
Stage IV Noise Margin	11.2	14.7	28.5	43.6	43.7	43.9
TOGW	656000	547286	464768	402859	396204	401240
OEW	320800	261889	227465	205666	204749	206470

TABLE 9. GEARED TURBOFAN ENGINE PERFORMANCE

	Baseline	2010	N+2 Tube and Wing	N+2 HWB with Podded Engines	N+2 HWB with Flush Mounted BLI Engines	N+2 HWB with Embedded BLI Engines
FPR	1.58	1.415	1.462	1.462	1.462	1.462
BPR	8.80	14.72	15.10	14.95	14.37	14.28
TSFC	0.5363	0.492	0.499	0.5021	0.5026	0.513
Engine Diameter	123	132.3	116.3	103	102.7	104.2
SLS Thrust	97300	79307	67109	53088	52363	52828
Engine Weight	16658	14223	9463	7196	7190	7422
LPC stages	3	2	2	2	2	2
LPT stages	6	4	4	4	4	4
Gear Ratio	1	2.1871	2.0871	2.0871	2.0871	2.0871
Fuel Burn	246329	193853	152479	117723	112150	114353
Stage IV Noise Margin	11.2	16.8	26.6	42.3	42.6	42.7
TOGW	656000	534809	452664	394574	387814	391406
OEW	320800	257780	220754	201289	200155	201007

Conclusions and Future Work

This paper presents an engine sizing and cycle selection study of ultra high bypass ratio engines applied to a subsonic commercial aircraft in the N+2 timeframe. Five test cases were used to demonstrate the change in engine performance with respect to different technologies, engine architecture, and airframe architecture. It was shown that a GTF had the potential to operate at lower fan pressure ratios than a direct drive engine offering both improvements in fuel burn and noise. In general, the N+2 technologies offer approximately 38% reduction in fuel burn and 20 dB increase in noise margin. The HWB potentially can offer

a further 23% fuel burn reduction and 15 dB noise margin. The flush mounted engine with boundary layer ingestion was shown to provide an additional 4.7% improvement in fuel burn relative to the podded case. Embedded engines in the HWB potentially can offer further reductions in fuel burn but it was demonstrated the design of a low loss inlet is critical in realizing these benefits, since even a 1% increase in total pressure loss can counteract the gains from reduced airframe drag.

Future work will be to extend this study to different size aircraft and engines as well as the exploration of which packages of technologies can be applied to simultaneously meet ERA fuel burn, noise, and emissions goals. This can be extended to a probabilistic assessments to quantify the risk in pursuing different technologies. These assessments will be used to perform fleet impact studies. Additionally the EDS environment can be used to study different bleed/cooling flow scheduling algorithms or an embedded engine sensitivity study to provide optimal performance and maximum operability. Other future work includes the integration of the "open rotor" engine technology into the EDS framework.

ACKNOWLEDGMENT

This work was funded by NASA through the National Institute of Aerospace under contract 6273-GT. The ERA project manager is Dr. Fay Collier, with day to day project oversight of the ASDL team by Mr. Craig Nickol. The authors would like to graciously thank all members of the ASDL ERA systems analysis team who have worked tirelessly on the project over the last year to complete all of the assessments.

REFERENCES

- [1] Collier, F., 2011. Status Update on Environmentally Responsible Aviation (ERA) Project. Integrated Systems Research Program Technical Sessions, 49th AIAA Aerospace Sciences Meeting, January.
- [2] Hupe, J., 2001. "Experts Reformulating Strategy for Alleviating Aviation's Impact on the Environment". *ICAO Journal*, **56**(4), June, pp. 5–7.
- [3] Gliebe, P., and Janardan, B., 2003. Ultra-High Bypass Engine Aeroacoustic Study. Tech. Rep. NASA/CR2003-212525, October.
- [4] Daggett, D., Brown, S., and Kawai, R., 2003. Ultra-Efficient Engine Diameter Study. Tech. Rep. NASA/CR2003-212309, May.
- [5] Kawai, R., Friedman, D., and Serrano, L., 2006. Blended Wing Body (BWB) Boundary Layer Ingestion (BLI) Inlet Configuration and System Studies. Tech. Rep. NASA/CR-2006-214534, December.
- [6] Plas, A., Sargeant, M., Crichton, D., Greitzer, E., Hynes, T., and Hall, C., 2007. "Performance of a Boundary Layer Ingesting (BLI) Propulsion System". In 45th AIAA Aerospace Sciences Meeting and Exhibit. AIAA 2007-450.
- [7] Hall, C., and Crichton, D., 2007. "Engine Design Studies for a Silent Aircraft". *Journal of Turbomachinery*, **129**, July, pp. 479–487.
- [8] Blanco, E., Hall, C., and Crichton, D., 2007. "Challenges in the Silent Aircraft Engine Design". In 45th AIAA Aerospace Sciences Meeting and Exhibit. AIAA 2007-454.
- [9] Crichton, D., Xu, L., and Hall, C., 2007. "Preliminary Fan Design for a Silent Aircraft". *Journal of Turbomachinery*, **129**, January, pp. 184–191.
- [10] Guynn, M., Berton, J., Fisher, K., Tong, M., and Thurman, R., 2009. Engine Concept Study for an Advanced Single-Aisle Transport. Tech. Rep. NASA/TM-2009-215784.
- [11] Tong, M., Jones, S., and Haller, W., 2009. Engine Conceptual Design Studies for a Hybrid Wing Body Aircraft. Tech. Rep. NASA/TM2009-215680, November.
- [12] Schutte, J., and Mavris, D., 2010. FY2010 Environmentally Responsible Aviation Systems Analysis Task 1 Report: Technology Portfolio and Advanced Configurations. Tech. rep., August.
- [13] Tong, M., 2007. A Probabilistic System Analysis of Intelligent Propulsion System Technologies. Tech. Rep. GT 2007-27914.
- [14] Tong, M., 2010. "An assessment of the impact of emerging high-temperature materials on engine cycle performance". In Proceedings of ASME Turbo Expo 2010: Power for Land, Sea and Air. GT2010-22361.
- [15] Hughes, C., and Zeug, T., 2008. NASA/GE Aviation Collaborative Partnership Research in Ultra High Bypass Cycle Propulsion Concepts. Fundamental Aeronautics Program 2nd Annual Meeting, October.
- [16] Hughes, C., Lord, W., and Masoudi, S., 2008. NASA/Pratt and Whitney Collaborative Partnership Research in Ultra High Bypass Cycle Propulsion Concepts. Fundamental Aeronautics Program 2nd Annual Meeting, October.
- [17] Kurzke, J., 2009. "Fundamental Differences Between Conventional And Geared Turbofans". In Proceedings of ASME Turbo Expo 2009: Power for Land, Sea and Air. GT2010-59745.
- [18] Kirby, M., and Mavris, D., 2008. "The Environmental Design Space". In 26th International Congress of the Aeronautical Sciences. ICAS-2008-4.7.3.
- [19] Converse, G., and Giffin, R., 1984. Extended Parametric Representation of Compressors Fans and Turbines. Vol. I - CMGEN User's Manual. Tech. Rep. NASA CR-174645, March.
- [20] Glassman, A., 1995. Design Geometry and Design/Off-Design Performance Computer Codes for Compressors and Turbines. Tech. Rep. NASA CR 198433.
- [21] Lytle, J., 1999. The Numerical Propulsion System Simulation: A Multidisciplinary Design for Aerospace Vehicles.

- Tech. Rep. NASA TM-1999-209194, September.
- [22] Lytle, J., 2000. The Numerical Propulsion System Simulation: An Overview. Tech. Rep. NASA TM-2000-209915, June.
- [23] Onat, E., and Klees, G., 1979. A Method to Estimate Weight and Dimensions of Large and Small Gas Turbine Engines. Tech. Rep. NASA-CR-159481, January.
- [24] Tong, M., Halliwell, I., and Ghosn, L., 2002. "A Computer Code for Gas Turbine Engine Weight and Disk Life Estimation". In 2002 ASME Turbo Expo. GT-2002-30500.
- [25] McCullers, L. *Flight Optimization System, Release 6.12, User's Guide*, Revised 14 October 2004 ed.
- [26] Development of the Technical Basis for a New Emission Parameter Covering the Whole AIRcraft Operation: NEPAIR - Final Technical Report. Tech. Rep. G4RD-CT-2000-00182, European Commission, September 2003.
- [27] Zorumski, W., 1982. Aircraft Noise Prediction Program Theoretical Manual, Part 1. Tech. Rep. NASA TM-83199-Pt-1, February.
- [28] Zorumski, W., 1982. Aircraft Noise Prediction Program Theoretical Manual, Part 2. Tech. Rep. NASA TM-83199-Pt-2, February.
- [29] Schutte, J., 2009. "Simultaneous multi-design point approach to gas turbine on-design cycle analysis for aircraft engines". PhD Thesis, Georgia Institute of Technology, Atlanta, GA, May.
- [30] Ballal, D., and Zelina, J., 2004. "Progress in Aeroengine Technology (1939-2003)". *JOURNAL OF AIRCRAFT*, **41**(1), February, pp. 43–50.
- [31] , 2010. Certificate data sheet: General electric company models: Genx-1b54 genx-1b58 genx-1b64 genx-1b67 genx-1b70, genx-2b67. Tech. Rep. E00078NE, Federal Aviation Administration.
- [32] Aungier, R., 2006. *Turbine Aerodynamics: Axial-flow and Radial-flow Turbine Design and Analysis*. ASME Press, New York.
- [33] Schutte, J., Jimenez, H., and Mavris, D., 2011. "Technology Assessment of NASA Environmentally Responsible Aviation Advanced Vehicle Concepts". In 49th AIAA Aerospace Sciences Meeting and Exhibit. AIAA 2011-6.
- [34] Nickol, C., and McCullers, L., 2009. "Hybrid Wing Body Configuration System Studies". In 47th AIAA Aerospace Sciences Meeting and Exhibit. AIAA 2009-931.
- [35] Tillman, G., and et. al., 2010. BLI Inlet and Distortion-Tolerant Fan Design. NASA Subsonic Fixed Wing Annual Review, October.
- [36] Felder, J., Kim, H., Brown, G., and Cho, J., 2011. "An Examination of the Effect of Boundary Layer Ingestion on Turboelectric Distributed Propulsion Systems". In 49th AIAA Aerospace Sciences Meeting and Exhibit. AIAA 2011-300.